The sound power output of a monopole source in a cylindrical pipe containing area discontinuities

Wenbo Duan, Ray Kirby

ACOUSTICS 2012

The sound power output of a monopole source in a cylindrical pipe containing area discontinuities

W. Duan and R. Kirby

Brunel University, Kingston Lane, Uxbridge, UB8 1PH Middlesex, UK
wenbo.duan@brunel.ac.uk

The sound power of a monopole source in free space is well known, and it is also known that the radiating sound power is not only determined by the source itself, but also the immediate environment surrounding the source. In this paper, a hybrid finite element method is used to study the sound power radiating from a monopole source placed close to a pipe discontinuity. It is found that while the sound power of a monopole source in free space increases as frequency squared, the sound power radiated from the same source in a cylindrical pipe is constant in the plane wave region. A sharp increase in sound power is then seen to occur when the first high-order mode cuts on; sound power is then seen to decrease as a function of frequency until the second high-order mode cuts on, and so on. It is also found that a wave reflected by a discontinuity placed close to one side of the source will interact with a wave on the other side travelling away from the source. This alters the sound power radiating from the source and has ramifications for the placement of monopole sources in piping systems.

1 Introduction

It is well known that sounding board can increase sound power output in musical instruments. Similar behaviour exists in a pipeline system, and is not well studied in the literature. The amount of sound power that travels into each branch is related to the relevant position of the sound source inside the system and has to be studied to achieve maximum sound power output. The reflections from the surrounding structure have a very complex interference with the acoustic source and will influence the total amount of sound power that is emitted by the sound source. This article investigates the effect of a blockage on the wave propagation in a pipe system which contains a monopole source. A hybrid finite element (FE) method is adopted here to model the problem by linking the different regions inside the pipe.

It is sometimes believed that the radiated sound power of a sound source is determined by the sound source only, and has nothing to do with its surroundings. It is not so for steady state sound field. A simple example is the output sound power of the monopole source near a rigid reflecting surface, which is doubled compared to the same source in the free space [1]. Reflections from the surrounds falling on a source, which are coherent with (phase related to) the source action, affect the sound power generated by that action [2]. The effect of the pipe wall and its non-uniform sections or terminations on the sound power output of a monopole source is not well studied in literature, due to the complex coherence pattern between the acoustic pressure and velocity. The wave propagation in a uniform duct containing a non-uniform section is studied by Astley [3]. Analytic modal expansions in the uniform section are coupled to the FE solutions in the non-uniform section of the pipe. Kirby [4] developed this hybrid FE method by allowing the modal solutions in the uniform section of the pipe to be obtained numerically. Thus, the model can be applied to a pipe with an arbitrary cross-section and contains one or more arbitrary non-uniform sections. Both mode matching [3, 4] and point collocation [5] can be used to enforce the continuity equations over different sections. However, in Astley's model, the source region is excluded and the acoustic pressure or its normal derivative has to be specified on a surface that surrounds the radiation region. In Kirby [4] and Kirby and Lawrie's articles [5], the source is represented by a sum of modes with known amplitudes. For a general sound field, for instance, the aeroacoustic sources associated with the fan of a gas turbine, the sources may by simulated by a distribution of elemental acoustic sources over a cross-section of the duct. Kim and Nelson [6] use the method of Green's function to model the modal amplitudes of a set of monopole sources in a cylindrical duct. The Green's function is expressed as a sum of modes in the duct, but the modal amplitudes cannot be solved directly and are related to the reflection coefficients of the reflected and incident waves. The reflection coefficients can only be solved separately by assuming that the upstream section is uncoupled to the source and the downstream section is anechoic. In this paper, we shall see that if the downstream section is not anechoic, then the upstream section is coupled to the source, since reflections from downstream section would affect the sound power radiated into the upstream section.

In this article, a hybrid FE method is used to join a region that encloses the source and a uniform regular region such as a pipe [3, 4]. The advantage of this method is that the inhomogeneous wave equation can be solved numerically, and fully coupled to the surrounding structures. The hybrid method avoids the need to mesh the uniform region, and thus greatly saves the computation memory, and speeds up the computation time. We study the sound power of a monopole source in an infinitely long cylindrical duct. Unlike the monopole source in free space, where the sound power increase as frequency squared, the sound power of the same source in a duct is constant in the plane wave region, until the high order mode cuts on.

A hybrid FE method which joins different regions, ie., a region that contains the source and a discontinuity region in the duct, is presented in Section 2. Finite element method is used to discretise the region that contains the source and the discontinuity region, while modal expansions are used for the uniform duct. The sound power radiated into different branches of the pipe is then studied in Section 3, and the conditions that can change the sound power output of the source are then analysed.

2 Theory

The monopole source is considered as an oscillating sphere of radius ϵ. The source strength of a monopole is defined as its surface area multiplied by its surface velocity [1]:

$$\boldsymbol{Q} = 4\pi\epsilon^2 U_\epsilon e^{i\omega t} = Q_s e^{i\omega t}. \quad (1)$$

where U_ϵ is the normal velocity amplitude on the surface of the oscillating sphere, $i = \sqrt{-1}$, ω is the radian frequency.

Relating the acoustic velocity to the source of mass, and taking the limit of small ϵ, the three-dimensional wave equation with a point source is given as:

$$\frac{1}{c^2}\frac{d^2p'}{dt^2} - \nabla^2 p' = i\omega\rho_0 Q_s e^{i\omega t}\delta(x-x_s)\delta(y-y_s)\delta(z-z_s) \quad (2)$$

where the delta (Dirac) function is defined as:

$$\delta(x-x_s)\delta(y-y_s)\delta(z-z_s) = 0 \text{ for } x \neq x_s, y \neq y_s \text{ and } z \neq z_s \quad (3)$$

and provided that Ω includes the source.

$$\int_\Omega \delta(x-x_s)\delta(y-y_s)\delta(z-z_s)\, d\Omega = 1.$$

The geometry of a monopole source in a pipe which also encloses a blockage is shown in Figure 1.

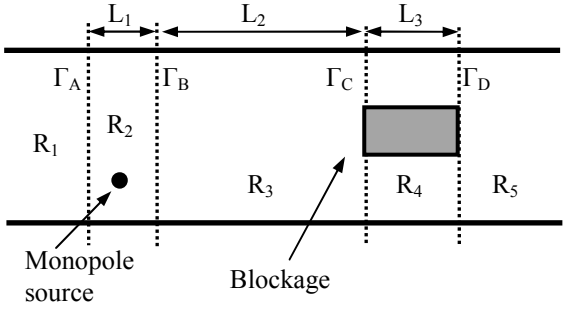

Figure 1. Monopole source in a pipe which encloses a blockage.

In region R_2, the governing equation is given as

$$-k^2 p_2 - \nabla^2 p_2 = F_2 \quad (4)$$

For region R_2 the acoustic pressure is approximated by

$$p_2(x,y,z) = \sum_{j=1}^{n_2} N_{2_j}(x,y,z) p_{2_j} = \mathbf{N_2 p_2}. \quad (5)$$

where N_{2_j} is a global trial (or shape) function for the finite element mesh in region R_2, p_{2_j} is the value of the sound pressure at node j, n_2 is the number of nodes in region R_2; and $\mathbf{N_2}$ and $\mathbf{p_2}$ are row and column vectors respectively. After applying Galerkin's method and Green's theorem, the governing equation in region R_2 is written as

$$\int_{\Omega_2}\left[\nabla \boldsymbol{N_2^T}\nabla \boldsymbol{N_2} - k^2 \boldsymbol{N_2^T N_2}\right] d\Omega_2 \boldsymbol{p_2} = \int_{\Gamma_2} \boldsymbol{N_2^T}\nabla p_2 \cdot n_2 d\Gamma_2 + \int_{\Omega_2} \boldsymbol{N_2^T} F_2\, d\Omega_2 \quad (6)$$

where

$$\int_{\Gamma_2} \boldsymbol{N_2^T}\nabla p_2 \cdot n_2 d\Gamma_2 = \int_{\Gamma_A} \boldsymbol{N_2^T}\nabla p_2 \cdot n_A d\Gamma_A + \int_{\Gamma_B} \boldsymbol{N_2^T}\nabla p_2 \cdot n_B d\Gamma_B + \int_{\Gamma_{2e}} \boldsymbol{N_2^T}\nabla p_2 \cdot n_{2e} d\Gamma_{2e} \quad (7)$$

For regions R_1 and R_3, the sound pressure field is given as:

$$p_1(x_1,y,z) = \sum_{n=0}^{m_1} A_n \Phi_n e^{ik\alpha_n x_1} \quad (8)$$

$$p_3(x_2,y,z) = \sum_{n=0}^{m_3} B_n \Phi_n e^{-ik\alpha_n x_2} + \sum_{n=0}^{m_3} C_n \Phi_n e^{ik\alpha_n x_2} \quad (9)$$

Continuity of pressure and velocity over Γ_A yields:

$$p_{2A} = \sum_{n=0}^{m_1} A_n \Phi_n \quad (10)$$

$$\frac{\partial p_{2A}}{\partial x} = ik\sum_{n=0}^{m_1} A_n \alpha_n \Phi_n \quad (11)$$

Continuity of pressure and velocity over Γ_B yields:

$$p_{2B} = \sum_{n=0}^{m_3} B_n \Phi_n + \sum_{n=0}^{m_3} C_n \Phi_n \quad (12)$$

$$\frac{\partial p_{2B}}{\partial x} = -ik\left\{\sum_{n=0}^{m_3} B_n \alpha_n \Phi_n - \sum_{n=0}^{m_3} C_n \alpha_n \Phi_n\right\} \quad (13)$$

Substituting Eqs. (11) and (13) into Eq. (7) yields,

$$\int_{\Gamma_2} \boldsymbol{N_2^T}\nabla p_2 \cdot n_2 d\Gamma_2 = -ik\int_{\Gamma_A} \boldsymbol{N_2^T}\sum_{n=0}^{m_1} A_n \alpha_n \Phi_n\, d\Gamma_A - ik\int_{\Gamma_B} \boldsymbol{N_2^T}\left[\sum_{n=0}^{m_3} B_n \alpha_n \Phi_n - \sum_{n=0}^{m_3} C_n \alpha_n \Phi_n\right] d\Gamma_B \quad (14)$$

The mode matching method is used to weight the pressure continuity Eqs. (10) and (12). Thus, Eqs. (10) and (12) yields,

$$ik\alpha_m \int_{\Gamma_A} \Phi_m \boldsymbol{N_2} d\Gamma_A \boldsymbol{p_{2A}} = ik\alpha_m \sum_{n=0}^{m_1} A_n \int_{\Gamma_A} \Phi_m \Phi_n d\Gamma_A \quad (15)$$

$$k\alpha_m \int_{\Gamma_B} \Phi_m N_2 d\Gamma_B\, p_{2B} = ik\alpha_m \sum_{n=0}^{m_3} B_n \int_{\Gamma_B} \Phi_m \Phi_n d\Gamma_B + ik\alpha_m \sum_{n=0}^{m_3} C_n \int_{\Gamma_B} \Phi_m \Phi_n d\Gamma_B \quad (16)$$

where $\mathbf{p_{2A}}$ and $\mathbf{p_{2B}}$ denotes values of the finite element solution in region R_2 at the nodal locations on the surface Γ_A and Γ_B respectively.

For regions R_4 and R_5, the sound pressure field is given as:

$$p_4(x_3,y,z) = \sum_{n=0}^{m_4} D_n \Psi_n e^{-ik\beta_n x_3} + \sum_{n=0}^{m_4} E_n \Psi_n e^{ik\beta_n x_3} \quad (17)$$

$$p_5(x_4,y,z) = \sum_{n=0}^{m_5} F_n \Phi_n e^{-ik\alpha_n x_4} \quad (18)$$

Mode matching technique is used to enforce continuity of pressure and velocity over Γ_C, which yields:

$$ik\beta_m \sum_{n=0}^{m_3} B_n \int_{\Gamma_C'} \Psi_m \Phi_n d\Gamma_C' e^{-ik\alpha_n L_2} + ik\beta_m \sum_{n=0}^{m_3} C_n \int_{\Gamma_C'} \Psi_m \Phi_n d\Gamma_C' e^{ik\alpha_n L_2} - ik\beta_m \sum_{n=0}^{m_4} D_n \int_{\Gamma_C'} \Psi_m \Psi_n d\Gamma_C' - ik\beta_m \sum_{n=0}^{m_4} E_n \int_{\Gamma_C'} \Psi_m \Psi_n d\Gamma_C' = 0 \quad (19)$$

$$-\sum_{n=0}^{m_3} B_n\, ik\alpha_n \int_{\Gamma_C} \Phi_m \Phi_n d\Gamma_C\, e^{-ik\alpha_n L_2}$$

$$+\sum_{n=0}^{m_3} C_n\, ik\alpha_n \int_{\Gamma_C} \Phi_m \Phi_n d\Gamma_C\, e^{ik\alpha_n L_2}$$

$$+\sum_{n=0}^{m_4} D_n\, ik\beta_n \int_{\Gamma_C'} \Phi_m \Psi_n d\Gamma_C'$$

$$-\sum_{n=0}^{m_4} E_n\, ik\beta_n \int_{\Gamma_C'} \Phi_m \Psi_n d\Gamma_C' = 0 \qquad (20)$$

Here, Γ_C' denotes the annulus region between the blockage and the pipe wall which lies on the surface of Γ_C. Similarly, continuity of pressure and velocity over Γ_D yields:

$$ik\beta_m \sum_{n=0}^{m_4} D_n \int_{\Gamma_D'} \Psi_m \Psi_n d\Gamma_D'\, e^{-ik\beta_n L_3}$$

$$+ik\beta_m \sum_{n=0}^{m_4} E_n \int_{\Gamma_D'} \Psi_m \Psi_n d\Gamma_D'\, e^{ik\beta_n L_3}$$

$$ik\beta_m \sum_{n=0}^{m_5} F_n \int_{\Gamma_D'} \Psi_m \Phi_n d\Gamma_D' = 0 \qquad (21)$$

$$-\sum_{n=0}^{m_4} D_n\, ik\beta_n \int_{\Gamma_D'} \Phi_m \Psi_n d\,\Gamma_D'\, e^{-ik\beta_n L_3}$$

$$+\sum_{n=0}^{m_4} E_n\, ik\beta_n \int_{\Gamma_D'} \Phi_m \Psi_n d\,\Gamma_D'\, e^{ik\beta_n L_3}$$

$$+\sum_{n=0}^{m_5} F_n\, ik\alpha_n \int_{\Gamma_D} \Phi_m \Phi_n d\Gamma_D = 0 \qquad (22)$$

Eq. (6), Eqs. (15)-(16) and Eqs. (19)-(22) are combined to give a final matrix equation as:

$$\begin{bmatrix} \mathbf{G_B} & \mathbf{G_{BC}} \\ \mathbf{G_{CB}} & \mathbf{G_{CC}} \end{bmatrix} \begin{Bmatrix} \mathbf{p_B} \\ \mathbf{p_C} \end{Bmatrix} = \begin{Bmatrix} \mathbf{f_B} \\ \mathbf{f_C} \end{Bmatrix} \qquad (23)$$

Here,

$$[\mathbf{G_B}] = \begin{bmatrix} -\mathbf{M_1} & \mathbf{Q_1} & \mathbf{0} & \mathbf{0} & \mathbf{0} \\ \mathbf{Q_1^T} & \mathbf{G_{2AA}} & \mathbf{G_{2Ae}} & \mathbf{G_{2AB}} & \mathbf{0} \\ \mathbf{0} & \mathbf{G_{2eA}} & \mathbf{G_{2ee}} & \mathbf{G_{2eB}} & \mathbf{0} \\ \mathbf{0} & \mathbf{G_{2BA}} & \mathbf{G_{2Be}} & \mathbf{G_{2BB}} & \mathbf{Q_3^T} \\ \mathbf{0} & \mathbf{0} & \mathbf{0} & \mathbf{Q_3} & -\mathbf{M_3} \end{bmatrix} \qquad (24)$$

$$[\mathbf{G_{BC}}] = \begin{bmatrix} \mathbf{0} & \mathbf{0} & \mathbf{0} & \mathbf{0} \\ \mathbf{0} & \mathbf{0} & \mathbf{0} & \mathbf{0} \\ \mathbf{0} & \mathbf{0} & \mathbf{0} & \mathbf{0} \\ -\mathbf{Q_3^T D_3} & \mathbf{0} & \mathbf{0} & \mathbf{0} \\ -\mathbf{M_3 D_3} & \mathbf{0} & \mathbf{0} & \mathbf{0} \end{bmatrix} \qquad (25)$$

$$[\mathbf{G_{CB}}] = \begin{bmatrix} \mathbf{0} & \mathbf{0} & \mathbf{0} & \mathbf{0} & \mathbf{M_{34} D_3} \\ \mathbf{0} & \mathbf{0} & \mathbf{0} & \mathbf{0} & -\mathbf{M_3^T D_3} \\ \mathbf{0} & \mathbf{0} & \mathbf{0} & \mathbf{0} & \mathbf{0} \\ \mathbf{0} & \mathbf{0} & \mathbf{0} & \mathbf{0} & \mathbf{0} \end{bmatrix} \qquad (26)$$

$$[\mathbf{G_{CC}}] = \begin{bmatrix} \mathbf{M_{34}} & -\mathbf{M_4} & -\mathbf{M_4 D_4} & \mathbf{0} \\ \mathbf{M_3^T} & \mathbf{M_{34}^T} & -\mathbf{M_{34}^T D_4} & \mathbf{0} \\ \mathbf{0} & \mathbf{M_4 D_4} & \mathbf{M_4} & -\mathbf{M_{54}} \\ \mathbf{0} & -\mathbf{M_{54}^T D_4} & \mathbf{M_{54}^T} & \mathbf{M_5^T} \end{bmatrix} \qquad (27)$$

$$\{\mathbf{p_B}\} = \begin{Bmatrix} \mathbf{A} \\ \mathbf{p_{2A}} \\ \mathbf{p_{2e}} \\ \mathbf{p_{2B}} \\ \mathbf{B} \end{Bmatrix} \qquad (28)$$

$$\{\mathbf{p_C}\} = \begin{Bmatrix} \tilde{\mathbf{C}} \\ \mathbf{D} \\ \tilde{\mathbf{E}} \\ \mathbf{F} \end{Bmatrix} \qquad (29)$$

$$\{\mathbf{f_B}\} = \begin{Bmatrix} \mathbf{0} \\ \mathbf{f_s} \\ \mathbf{0} \\ \mathbf{0} \\ \mathbf{0} \end{Bmatrix} \qquad (30)$$

$$\{\mathbf{f_C}\} = \begin{Bmatrix} \mathbf{0} \\ \mathbf{0} \\ \mathbf{0} \\ \mathbf{0} \end{Bmatrix} \qquad (31)$$

$[\mathbf{D_3}]$ and $[\mathbf{D_4}]$are diagonal matrices with each diagonal element given by $e^{-ik\alpha_n L_2}$, $(n = 0,1,\cdots,m_3)$ and $e^{-ik\beta_n L_3}$, $(n = 0,1,\cdots,m_4)$,respectively. $[\mathbf{D_3}]^{-1}\{\mathbf{C}\} = \{\tilde{\mathbf{C}}\}$, and $[\mathbf{D_4}]^{-1}\{\mathbf{E}\} = \{\tilde{\mathbf{E}}\}$. In addition,

$$\{\mathbf{f_s}\} = \sum_{j=1}^{n_s} \varepsilon_{sj}\, \omega\rho_0 Q_{sj} \mathbf{N_2^T}(x_{sj}, y_{sj}, z_{sj}) \qquad (32)$$

$$[\mathbf{G_2}] = \int_{\Omega_2} \left[\nabla \boldsymbol{N_2^T} \nabla \boldsymbol{N_2} - k^2 \boldsymbol{N_2^T N_2}\right] d\Omega_2 \qquad (33)$$

$$[\mathbf{Q_1}] = ik\alpha_m \int_{\Gamma_A} \Phi_m \boldsymbol{N_2} d\Gamma_A \quad (m = 0,1,\cdots,m_1) \qquad (34)$$

$$[\mathbf{Q_3}] = ik\alpha_m \int_{\Gamma_B} \Phi_m \boldsymbol{N_2} d\Gamma_B \quad (m = 0,1,\cdots,m_3) \qquad (35)$$

$$[\mathbf{M_1}] = ik\alpha_m \int_{\Gamma_A} \Phi_m \Phi_n d\Gamma_A$$
$$(m = 0,1,\cdots,m_1; n = 0,1,\cdots,m_1) \qquad (36)$$

$$[\mathbf{M_3}] = ik\alpha_m \int_{\Gamma_B} \Phi_m \Phi_n d\Gamma_B$$
$$(m = 0,1,\cdots,m_3; n = 0,1,\cdots,m_3) \qquad (37)$$

$$[M_{34}] = ik\beta_m \int_{\Gamma_C'} \Psi_m \Phi_n d\Gamma_C'$$
$$(m = 0,1,\cdots,m_4; n = 0,1,\cdots,m_3) \qquad (38)$$

$$[M_4] = ik\beta_m \int_{\Gamma_C'} \Psi_m \Psi_n d\Gamma_C'$$
$$(m = 0,1,\cdots,m_4; n = 0,1,\cdots,m_4) \qquad (39)$$

$$[M_{54}] = ik\beta_m \int_{\Gamma_D'} \Psi_m \Phi_n d\Gamma_D'$$
$$(m = 0,1,\cdots,m_4; n = 0,1,\cdots,m_5) \qquad (40)$$

$$[M_5] = ik\alpha_m \int_{\Gamma_D} \Phi_m \Phi_n d\Gamma_D$$
$$(m = 0,1,\cdots,m_5; n = 0,1,\cdots,m_5) \qquad (41)$$

Matrix $[\mathbf{G_2}]$ is decomposed into separate elements to give

$$[\mathbf{G_2}]\mathbf{p_2} = \begin{bmatrix} \mathbf{G_{2AA}} & \mathbf{G_{2Ae}} & \mathbf{G_{2AB}} \\ \mathbf{G_{2eA}} & \mathbf{G_{2ee}} & \mathbf{G_{2eB}} \\ \mathbf{G_{2BA}} & \mathbf{G_{2Be}} & \mathbf{G_{2BB}} \end{bmatrix} \begin{Bmatrix} \mathbf{p_{2A}} \\ \mathbf{p_{2e}} \\ \mathbf{p_{2B}} \end{Bmatrix} \quad (42)$$

In the above equations, matrix $[\mathbf{G_B}]$ has the order $(n_2 + m_1 + m_3) \times (n_2 + m_1 + m_3)$. matrix $[\mathbf{G_{BC}}]$ has the order $(n_2 + m_1 + m_3) \times (m_3 + 2m_4 + m_5)$. Matrix $[\mathbf{G_{CB}}]$ has the order $(m_3 + 2m_4 + m_5) \times (n_2 + m_1 + m_3)$. matrix $[\mathbf{G_{CC}}]$ has the order $(m_3 + 2m_4 + m_5) \times (m_3 + 2m_4 + m_5)$. $\{\mathbf{p_B}\}$ and $\{\mathbf{f_B}\}$ are the vectors of order $(n_2 + m_1 + m_3)$. $\{\mathbf{p_C}\}$ and $\{\mathbf{f_C}\}$ are the vectors of order $(m_3 + 2m_4 + m_5)$.

3 Results and discussion

The results obtained from the numerical models described in the previous section are presented in the form of sound power. In the calculations that follow, the fluid in all regions is assumed to be air, in which the speed of sound $c = 343.2244$ m/s.

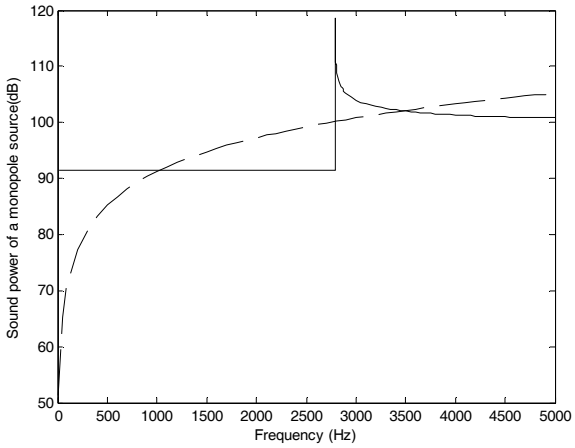

Figure 2. Sound power radiated by a monopole source. ——— source in the pipe; – – – : source in the free space.

Fig. 2 shows the comparison of the calculated sound power between a monopole source in a cylindrical pipe and the same source in the free space. The radius of the pipe is *a=75* mm. The radius of the blockage is zero in this case, which means that no blockage is present. Note that the sound power in the pipe in Fig. 2 is the total sound power radiated into regions R_1 and R_3. Since the pipe is symmetric about the source plane, the source radiates equally into regions R_1 and R_3. The monopole source is placed on the central axis of the pipe, so the circumferential high-order modes won't be excited. The first radial high-order mode will cut on at 2791Hz. It can be seen from Fig. 2 that the sound power in the pipe is largely mode dependent, and in the plane wave region the sound power is a constant. In the free space, the total sound power increases as frequency squared. So in the low frequency region, the monopole source radiates more power in the pipe than in the free space, but in the high frequency range, the situation can be inversed. At cut-on frequency, the first radial mode radiates infinity sound power into the pipe if assuming no damping is present. Above the cut-on frequency, the plane wave still radiates the same amount of sound power as in the plane wave region, although the first radial high-order mode will be a more efficient sound power radiator than the plane wave mode. Unlike the monopole source in the free space, the sound power will decrease with frequency increases, until the second high-order mode cuts on, and then the similar behaviour will continue. A number of numerical experiments using different pipe radius reveal that the total sound power of a monopole source in a cylindrical pipe in the plane wave region is related to the area of the pipe only, and is given as,

$$\Pi_{tr} = \frac{Q_S^2 \rho_0 c}{4\pi a^2}, \quad (43)$$

where Eq. (43) is valid irrespective of the position of the source in the pipe. Of course, this result is well known [7] and serves to validate the predictions generated here. The real power of the model presented here is in the study of high-order circumferential or radial mode cuts on, where the position of the source will matter.

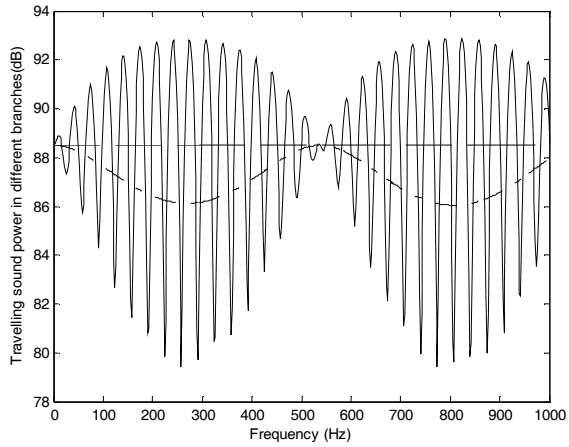

Figure. 3. Sound power in pipe with blockage. ———, sound power in R_1; , — — - sound power in R_3; — · — · — sound power in R_5.

Fig. 3 shows the sound power radiated into different branches of a pipe which contains a blockage. A monopole source is placed on the central axis of the pipe. The blockage is 300mm long, 55mm in radius, and 5m away from the source. The sound power radiated into region R_3 is a constant, and is half the value given in Eq. (43). Then part of this power will be reflected back into the left hand side of the pipe, and part of this power will be transmitted into region R_5. So the radiated power in region R_5 is always less than or at most equal to the power radiated into region R_3. The specific reflection and transmission power ratio is related to the geometric shape of the blockage, and will not be detailed here. It is interesting to note that the sound power radiated into region R_1 exhibits an oscillatory behaviour. This is because that the initial wave omitted by the source into the left hand side of the pipe interacts with the reflected wave from the blockage, and forms an interference pattern in region R_1. The total sound power in region R_1 is thus determined not only by the phase difference between the initial wave from the source and the reflected wave from the blockage, but also by the magnitude of the reflected wave. It is clear that when the power radiated into region R_5 is low. Then the reflected power from the blockage will be high, and the maximum power radiated into region R_1 will be high as well. The period of the oscillation pattern of the power radiated into region R_1 is related to the distance between the source and

the blockage. Suppose this distance is D, then at a frequency f_1, the number of wavelengths that the wave travels from the source to the blockage, and is then reflected back to the source is given as: $2D/\lambda_1 = 2Df_1/c$, where λ_1 is the wavelength. At a different frequency f_2, the number of wavelengths will be $2Df_2/c$. If $2Df_2/c - 2Df_1/c = 1$, which indicates that the wave has travelled one more wavelength, and the phase difference between the initial wave from the source and the reflected wave from the blockage at these two frequencies will be the same. It is thus deduced that the period of the oscillation of the sound power travelled into region R_1 is $\Delta f = c/2D$.

4 Conclusion

A hybrid numerical method is used to study the sound power output of a monopole source in a cylindrical pipe. The hybrid method allows the inhomogeneous wave equation to be solved directly, and coupled to the other homogenous wave fields. The hybrid method meshes only the discontinuity region in the duct and the region that surrounds the source, thus greatly saves computation memory and speeds up the computation time. If a blockage is placed in the downstream of the duct, then the reflected wave from the blockage will interact with the initial wave from the source that radiates into the upstream of the duct. The result is that the downstream power is determined by the source only, while the upstream power is determined by coupling between the source and the reflected wave from the blockage. The oscillation power in the upstream region is found to be also related to the distance between the source and the blockage.

Acknowledgments

The authors would like to thank the UK Engineering and Physical Sciences Research Council (EPSRC) for their support of the work reported in this article.

References

[1] M.P. Norton, *Fundamentals of noise and vibration analysis for engineers*. Cambridge: Cambridge University Press. 1989.

[2] F.J. Fahy, *Sound intensity*. 2nd ed.: E & FN Spon. 1995.

[3] R.J. Astley, Fe mode-matching schemes for the exterior helmholtz problem and their relationship to the fe-dtn approach. *Comm. Num. Meth. Eng.*, 1996. **12**(4): p. 257-267.

[4] R. Kirby, Modeling sound propagation in acoustic waveguides using a hybrid numerical method. *J. Acoust. Soc. Am.*, 2008. 124(4): p. 1930-1940.

[5] R. Kirby, and J.B. Lawrie, A point collocation approach to modelling large dissipative silencers. *J. Sound Vib.*, 2005. 286(1-2): p. 313-339.

[6] Y. Kim, and P.A. Nelson, Estimation of acoustic source strength within a cylindrical duct by inverse methods. *J. Sound Vib.*, 2004. **275**(1-2,): p. 391-413.

[7] A. Pierce, *Acoustics, an introduction to its physical principles and applications*. Mc Graw Hill, New York, 1981.